


Stability, Mechanical Properties and Anisotropic Elastic Properties of Ga_xMg_y Compounds

LinJing Liu^a, Liangchong Lian^a, Jie Yu^{b*}

^aDepartment of Mechanical and Electrical Engineering, Hunan Biological and Electromechanical Polytechnics, Changsha, 400126, China

^bFaculty of Material Science and Engineering, Kunming University of Science and Technology, Kunming, 650093, China

Received: September 19, 2018; Revised: November 19, 2018; Accepted: November 20, 2018

The stability, mechanical properties and anisotropic properties of sound velocities of Ga₂Mg₅, GaMg₂, GaMg, O-Ga₂Mg, H-Ga₂Mg and Ga₃Mg₂ are investigated systematically by the first-principles calculation. The cohesive energy and formation enthalpy are obtained and used to estimate the stability of the Ga-Mg binary compounds. GaMg compound is the most stable and has the lowest formation enthalpy as -0.162eV/atom of those Ga_xMg_y compounds. The elastic constants of single crystal, hardness, bulk, shear, Young's modulus and Poisson's ratio of the polycrystalline crystal are obtained and used to estimate the mechanical properties. Ga₃Mg₂ and H-Ga₂Mg have the larger bulk, shear and Young's modulus and corresponding B/G is low. H-Ga₂Mg is harder than the other compounds from the results of Poisson's ratio. The anisotropic mechanical properties are discussed using the anisotropic index, two-dimensional planar projections on different planes of the bulk and Young's modulus. The Young's modulus of H-Ga₂Mg shows the strongly anisotropy of mechanical properties and GaMg₂ has the weakest anisotropy among all the compounds.

Keywords: Gallium alloy, First-principle calculation, Mechanical properties, Anisotropy.

1. Introduction

Pure gallium is a soft metal with a low temperature melting point of 29.8 °C, in recent years, gallium is mainly used in liquid metal alloys with a variety of applications, including chip cooling¹⁻⁴, waste heat recovery^{5,6}, electrical interconnects and contacts^{7,8}, biomedical equipment⁹, kinetic energy harvesting¹⁰, thermal interface material^{11,12} or printed electronics¹³⁻¹⁶. The eutectic gallium-indium binary alloy (EGaIn 75% gallium and 25% indium) and gallium-indium-tin ternary alloy (Galinstan 68.5% gallium, 21.5% indium, 10% tin) are the most common used non-toxic liquid metals today and also gallium rich Pd-Ga phases as supported liquid metal catalysts¹⁷. Due to the particular characteristics of gallium, the addition of other elements to the gallium alloy will open up new possibilities for design and applications, such as magnesium. Ga-Mg alloy for sacrificial anodes in seawater batteries^{18,19}, hydrogen storage²⁰ and medical implants^{21,22}. In Ga-Mg alloys, the effect of secondary phases (Mg₃Ga₂) and impurities on the localized corrosion mechanism using AFM/SKPFM is also studied²³. However, the fundamental number of studies on Ga-Mg alloys is rather limited. There is some very early work regarding the phase diagram Ga-Mg summarized by Beck²⁴, which was updated by Nayeb-Hashemi et al.²⁵, Feng²⁶ and Meng²⁷. Thermodynamics is the key component of Ga-Mg alloy, one of critically important thermodynamic data is the enthalpy of formation of the compounds, which can be obtained by first-principles calculations²⁸.

To better control the design of a material with the desired properties, the thermodynamics and mechanical properties of gallium alloys are very necessary. In this work, the cohesive energy, formation enthalpy, mechanical properties and anisotropic elastic properties for all the Ga-Mg binary compounds based on Ga-Mg phase diagram are investigated by first principle calculations. The thermodynamic database and mechanical properties for the Ga-Mg system is helpful for the design of Gallium alloys.

2. Methods and Details

In this work, the whole calculations are carried out by first principle calculations which are based on density functional theory (DFT) as implemented in Cambridge sequential total energy package (CASTEP) code²⁹⁻³¹. The crystal structures are optimized by a plane wave expansion method. By comparing ultrasoft and Norm-conserving pseudo potentials (NCPPs), NCPPs are used to indicate the interactions between ionic core and valence electrons. The exchange correction energy is calculated by the generalized gradient-corrected (GGA) developed by Perdew, Burke and Ernzerhof (PBE)³². Monkhorst-Pack scheme is used for k-point sampling in the first irreducible Brillouin zone³³. The 4s²4p¹ and 3s² are considered as valence electrons configurations for Ga and Mg, respectively. The Brillouin zone is sampled with the Monkhorst-Pack scheme³³ and the K point mesh is selected as 5×5×5 for all structures. The maximum energy cut off value of 450.0 eV is used for plane wave expansion

*e-mail: yujieone@163.com

in reciprocal space. The total energy changes during the optimization process are reduced to 1×10^{-6} eV and the forces acting on distinct atom are converged to 0.05 eV/Å.

In order to estimate the thermodynamic stability of Ga_xMg_y compounds, the cohesive energy and formation enthalpy were calculated in this paper. The following expressions (Eq.(1) and Eq.(2)) were estimated as following equations:

$$E_{coh}(Ga_xMg_y) = \frac{E_{tot}(Ga_xMg_y) - xE_{iso}(Ga) - yE_{iso}(Mg)}{x + y} \quad (1)$$

$$\Delta H_f(Ga_xMg_y) = \frac{E_{tot}(Ga_xMg_y) - xE_{bin}(Ga) - yE_{bin}(Mg)}{x + y} \quad (2)$$

Where, $E_{coh}(Ga_xMg_y)$ and $\Delta H_f(Ga_xMg_y)$ are the cohesive energy and formation enthalpy of Ga_xMg_y per atom, respectively; $E_{tot}(Ga_xMg_y)$ is the total cell energy of Ga_xMg_y phase; E_{iso} refers to the total energy of an isolated Ga or Mg atom and E_{bin} is the cohesive energy of crystal of Ga or Mg, respectively. The elastic constants of compounds in Ga_xMg_y were calculated by stress-strain method, within namely Hooker's law. Several different strain modes were imposed on the crystal structure, and the Cauchy stress tensor for each strain mode was evaluated. Finally, the related elastic constants were identified as the coefficients in strain-stress relations as shown in Eq. (3)³⁴:

$$\begin{pmatrix} \sigma_1 \\ \sigma_2 \\ \sigma_3 \\ \tau_4 \\ \tau_5 \\ \tau_6 \end{pmatrix} = \begin{pmatrix} C_{11} & C_{12} & C_{13} & C_{14} & C_{15} & C_{16} \\ & C_{22} & C_{23} & C_{24} & C_{25} & C_{26} \\ & & C_{33} & C_{34} & C_{35} & C_{36} \\ & & & C_{44} & C_{45} & C_{46} \\ & & & & C_{55} & C_{56} \\ & & & & & C_{66} \end{pmatrix} \begin{pmatrix} \varepsilon_1 \\ \varepsilon_2 \\ \varepsilon_3 \\ \gamma_4 \\ \gamma_5 \\ \gamma_6 \end{pmatrix} \quad (3)$$

where, C_{ij} is the elastic constant, τ_i and σ_i are the shear stress and normal stress, respectively. The total number of independent elastic constants is determined by the symmetry of the crystal. In high symmetry system, the indispensable different strain patterns for the C_{ij} calculations can be greatly reduced.

3. Results and Discussion

3.1 Stability

Fig. 1 illustrates the Ga-Mg equilibrium phase diagram³⁵, in this phase diagram, the crystal structures of gallium magnesium including Ga_2Mg_5 , $GaMg_2$, $GaMg$, Ga_2Mg , and Ga_3Mg_2 are prepared from reference. For Ga_2Mg , there are two polymorph structures, orthorhombic and hexagonal³⁶, which are marked as O- Ga_2Mg and H- Ga_2Mg respectively. The other compounds contain three different types of lattice-tetragonal (Ga_3Mg_2 and $GaMg$), orthorhombic (Ga_2Mg_5) and hexagonal ($GaMg_2$) crystal classes. Fig.2 shows the crystal structures of the Ga-Mg binary system. The calculated lattice

parameters of optimized crystal structures and the described chemical stability of the intermetallic compounds of Ga-Mg binary system by cohesive energy and formation enthalpy are demonstrated in Table 1. Obviously, the crystal parameters of Ga-Mg compounds are in good agreement with other calculated values and experimental results. The calculated results are obtained at 0 K, but the experimental results are measured at room temperature. Moreover, when different exchange-correlation functions are used, the lattice parameters may be underestimated or overestimated. Therefore, the tiny deviation may result from the influence of thermodynamic effect on the crystal structure. The stability of the Ga-Mg binary compounds can be determined by cohesive energies and formation enthalpies. The results calculated by Eq. (1) and (2) are also tabulated in Table 1, the values of cohesive energy and formation enthalpy are negative. However, the chemical stability of Ga-Mg system compounds is determined by formation enthalpy. The lower the formation enthalpy, the more stable the compound. It can be seen that the formation enthalpy of GaMg (-0.162 eV/atom) is the lowest value, and indicating the most stable phase is GaMg in the Ga-Mg binary compounds. On the other hand, Ga_2Mg_5 has the highest formation enthalpy as -0.120 eV per atom, implying that it is less stable than other Ga_xMg_y compounds. With the increase of Ga concentration in Ga_xMg_y , the cohesive energy increasing, and the maximum and minimum value is -1.858 eV/atom and -3.701 eV/atom for α -Mg and α -Ga; respectively. Fig.3 depicts the calculated and previously reported formation enthalpy of Ga_xMg_y compounds. The calculated values in this work are in consistent with the available experimental data in Ref.^{37,38} Because of different approximation method resulting in calculation accuracy, the values are a little difference with the values obtained by Hui Zhang et al²⁸, and in Ref.^{28,37,38} the enthalpy of formation is expressed as kJ/mol, we calculated the enthalpy of formation expresses as eV/atom. The stability of these compounds forms the following sequence: $GaMg > O-Ga_2Mg > H-Ga_2Mg > Ga_3Mg_2 > GaMg_2 > Ga_2Mg_5$. In a word, GaMg is the most stable compound among Ga-Mg binary system.

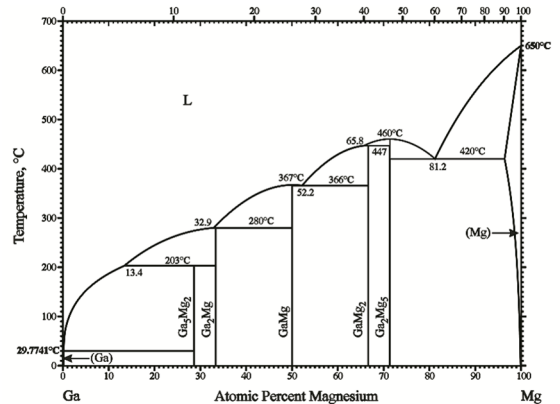


Figure 1. The Ga-Mg equilibrium phase diagram.

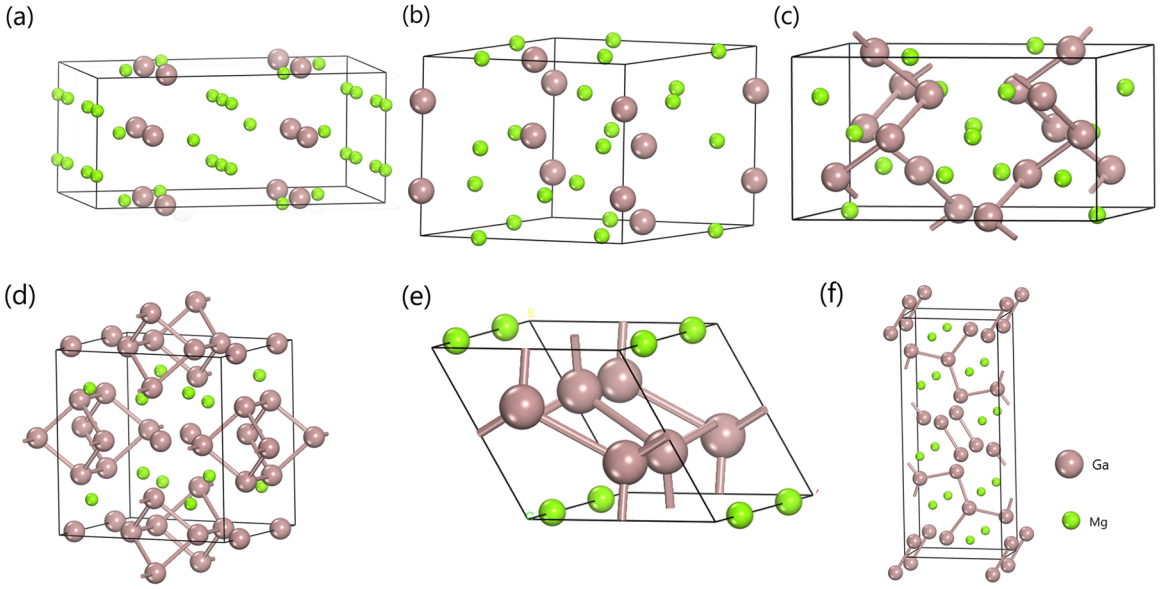


Figure 2. The crystal structures of the Ga-Mg binary system. (a) Ga₂Mg₅; (b) GaMg₂; (c) GaMg; (d) Ga₃Mg₂; (e) H-Ga₂Mg; (f) O-Ga₂Mg₅.

Table 1. The Lattice parameters (a , b and c), cohesive energy (E_{coh}) and formation enthalpy (ΔH_f) of Ga-Mg binary compounds.

Species	Space group	Composition at.% Ga	Lattice constants (Å)			E_{coh} (eV/ atom)	ΔH_f (eV/atom)
			a	b	c		
α -Mg	P63/mmc	0	3.209	3.209	5.211	-1.858	0
Ga ₂ Mg ₅	Ibam	28.57	7.004b	13.663b	5.987b	-2.504b	-0.120b
			7.017g	13.708g	6.020g		-0.113i
			7.036c	13.747c	6.028c		-0.119c
GaMg ₂	P-62c	33.33	7.730b	7.730b	6.976b	-2.605b	-0.133b
			7.794f	7.794f	6.893f		-0.121i
			7.805c		6.941c		-0.130c
GaMg	I41/aZ	50.00	10.523b	10.523b	5.539b	-2.941b	-0.162b
			10.530e		5.530e		-0.135i
			10.690c		5.555c		-0.142c
H-Ga ₂ Mg	P63/mmc	66.67	4.370b	4.370b	6.692b	-3.229b	-0.144b
			4.343h	4.343h	6.982h		
O-Ga ₂ Mg	Pbam	66.67	6.813b	16.259b	4.040b	-3.234b	-0.148b
			6.802a	16.346a	4.111a		-0.118i
			6.868c	16.457c	4.139c		-0.120c
Ga ₃ Mg ₂	I4/mmm	71.43	8.568b	8.568b	7.125b	-3.313b	-0.140b
			8.627d		7.111d		-0.103i
			8.725c	8.725c	7.178c		-0.112c
α -Ga	Cmca	100	3.706 4	4.8891	7.971	-3.701	0

^aExp. In Ref.³⁹

^bThis work

^cCal. In Ref.²⁸

^dExp. In Ref.⁴⁰

^eExp. In Ref.⁴¹

^fExp. In Ref.⁴²

^gExp. In Ref.⁴³

^hExp. In Ref.⁴⁴

ⁱExp. In Ref.³⁷

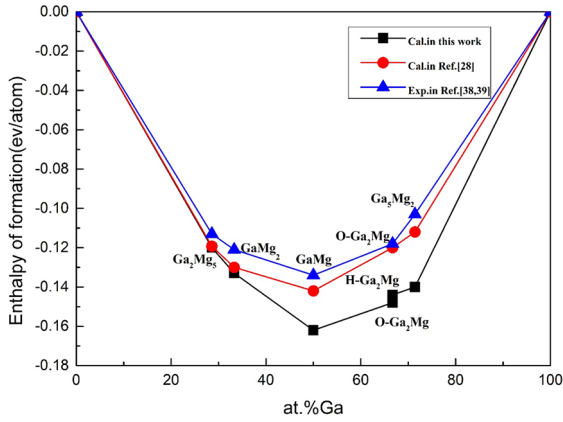


Figure 3. Calculated enthalpies of formation plotted as a function of composition for the Ga-Mg system.

3.2 Mechanical properties

The response of crystals to external forces is determined by elastic constants, which is of great significance in practical applications. Therefore, it is necessary to study the elastic constants of Ga-Mg binary compounds for the mechanical properties. The elastic constants of Ga_xMg_y compounds are determined by Eq. (3) based on the generalized Hook's law⁴⁵, and the results are summarized in Table 2. According to Born-Huang's mechanical stability criterions, one condition is the strain energy must be positive for any homogeneous elastic deformation. The mechanical stability criterions can be expressed as⁴⁶:

Tetragonal system:

$$\begin{aligned} C_{11} > 0, C_{33} > 0, C_{44} > 0, C_{66} > 0, C_{11} - C_{12} > 0, \\ C_{11} + C_{33} - C_{13} > 0, 2(C_{11} + C_{12}) + C_{33} + 4C_{13} > 0, \end{aligned} \quad (4)$$

Orthorhombic system:

$$\begin{aligned} C_{11} + C_{12} + C_{33} + 2C_{12} + 2C_{23} > 0, \\ C_{11} + C_{22} > 2C_{12}, C_{22} + C_{33} > 2C_{33}, \\ C_{11} + C_{33} > 2C_{13}, C_{ii} > 0 (i = 1 - 6) \end{aligned} \quad (5)$$

Hexagonal system:

$$C_{11} > 0, C_{44} - C_{22} > 0, (C_{11} + C_{12})C_{33} > 2C_{13}^2 \quad (6)$$

As shown in Table 2, the values of elastic constants satisfied the above criterions, which imply all the Ga-Mg binary compounds are elastically stable. H-Ga₂Mg own the largest C_{11} value as 136.9 GPa, which shows that H-Ga₂Mg has high incompressibility under uniaxial stress along the crystallographic a axis (ϵ_{11}). O-Ga₂Mg has the largest C_{22} value as 102.8 GPa and Ga₅Mg₂ has the largest C_{33} value as 137.1 GPa, which shows that O-Ga₂Mg and Ga₅Mg₂ have high incompressibility under uniaxial stress along the crystallographic b axis (ϵ_{22}) and c axis (ϵ_{33}). C_{44} , C_{55} and C_{66} represent the shearing modulus on (100), (010) and (001) crystal plane, respectively. Ga₅Mg₂ and O-Ga₂Mg show the largest C_{44} 40.1 GPa and smallest C_{44} 23.9 GPa, the shearing strength of O-Ga₂Mg at (100) and (010) planes is weaker than (001) plane, while Ga₂Mg₅ shows the largest shearing strength at (100) plane.

The mechanical modulus such as bulk modulus (B), Young's modulus (E) and shear modulus (G) are evaluated by the elastic constants using Voigt-Reuss-Hill (VRH) approximation. The Voigt-Reuss-Hill (VRH) approximation is an average of Voigt and Reuss approximations, namely the upper and lower bounds to the elastic modulus, which provides the estimation for the mechanical properties of poly-crystalline materials from the known elastic constants for single crystal. Yong's modulus (E) and Poisson's ratio (σ) are estimated by following expressions⁴⁷⁻⁵⁰:

$$B_{VRH} = \frac{1}{2}(B_V + B_R) \quad (7)$$

$$G_{VRH} = \frac{1}{2}(G_V + G_R) \quad (8)$$

$$E = \frac{9B_{VRH}G_{VRH}}{3B_{VRH} + G_{VRH}} \quad (9)$$

Table 2. The calculated elastic constants (C_{ij} , in GPa) of Ga-Mg system.

	α -Mg	Ga ₂ Mg ₅	GaMg ₂	GaMg	H-Ga ₂ Mg	O-Ga ₂ Mg	Ga ₅ Mg ₂	α -Ga
C_{11}	80.9	93.3	88.2	90.1	136.9	69.1	114.6	125.6
C_{22}	-	80.7	-	-	-	102.8	-	93.8
C_{33}	101.7	72.9	71.9	96.2	133.0	78.0	137.1	127.7
C_{44}	47.2	37.9	25.6	36.5	29.5	23.9	40.1	12.2
C_{55}	-	30.2	-	-	-	22.1	-	21.22
C_{66}	-	23.9	-	21.7	-	29.3	34.6	16.8
C_{12}	20.1	26.6	31.2	30.0	34.0	37.2	47.6	115.8
C_{13}	1.1	27.2	31.1	35.7	16.8	56.6	20.4	26.1
C_{23}	-	31.2	-	-	-	34.8	-	43.3
C_{16}				4.3			0	

$$\sigma = \frac{3B_{VRH} - 2G_{VRH}}{2(3B_{VRH} + G_{VRH})} \quad (10)$$

Here, B_V , B_R and B_{VRH} are the bulk modulus calculated by Voigt, Reuss and Voigt-Reuss-Hill approximation method, respectively. G_V , G_R and G_{VRH} are the shear modulus calculated within Voigt, Reuss and Voigt-Reuss-Hill approximation method, respectively. In this paper, we also calculated the first order Lamé constant (λ) and the second Lamé constant (μ), namely compressibility and shear stiffness, using the following expressions³¹:

$$\lambda = \frac{\sigma E}{(1 + \sigma)(1 - 2\sigma)} \quad (11)$$

$$\mu = \frac{E}{2(1 + \sigma)} \quad (12)$$

The related calculated values of Ga_xMg_y binary compounds are showed in Table 3, and Fig.4 illustrates the variations of elastic parameters of Ga_xMg_y compounds. The greater B values of Ga₅Mg₂ and H-Ga₂Mg than other compounds; indicate that Ga₅Mg₂ and H-Ga₂Mg are the most difficult to be compressed under hydrostatic pressure in the Ga-Mg binary compounds, which is in consistent with the analysis of elastic constants. In addition, the bulk modulus of Ga is significantly larger than Mg. With the increase of Ga content, the bulk modulus of Ga-Mg alloy also increased, except O-Ga₂Mg. Meanwhile, the G and E of Ga₅Mg₂ and H-Ga₂Mg are also larger than other compounds. The higher shear modulus is, the higher hardness of the compounds⁵². Because the intrinsic hardness is proportional to the shear modulus, the high hardness may correspond to Ga₅Mg₂ and H-Ga₂Mg. The ratio of B/G is used as an indicator for the ductility or brittleness of the compound; If the B/G values for the Ga_xMg_y binary compounds are lower than the critical value as 1.75, the compounds are brittle. O-Ga₂Mg has the

largest B/G value as 2.71, while H-Ga₂Mg has the lowest B/G value as 1.41 among the Ga-Mg binary compounds. The Vickers hardness (H_v) of Ga-Mg system is predicted by an empirical model which has better results for the anisotropic structures. The model is recently proposed by Chen et al. and expressed as follows⁵³:

$$H_v = 2(k^2 G)^{0.585} - 3 \quad (13)$$

Where k denotes the Pugh's modulus ratio ($k = G/B$). The hardness of H-Ga₂Mg is 9.05 GPa which is the largest in Ga-Mg system, while the value for O-Ga₂Mg is 0.66 GPa as the smallest one among the Ga-Mg system. In Fig. 4, the B/G value is multiplied by the factor of 5 and Poisson's ratio is multiplied by the factor of 20 for a better illustration. The shear modulus decreases firstly and then increases when the atom percent of Ga exceed 30%. A sharp peak occurs at Ga 66.7 at% on the curve which presents the maximum shear modulus value for H-Ga₂Mg, however, the minimum shear modulus value for O-Ga₂Mg, simultaneously. With the Ga atom content increasing, the variation of shear modulus has the same tendency as the variation of Young's modulus and Vickers hardness. Furthermore, the hardness may be more sensitive to shear modulus than bulk modulus. As shown in Fig. 4, the trend of the B/G value curve is the same as the Poisson's ratio with increasing Ga atom content. However, the trend of Poisson's ratio and Vickers hardness are opposite.

3.3 Anisotropy of elastic properties

The anisotropy of mechanical properties is very important in the application of materials. The occurrence of micro-cracks in materials is often related to the elastic anisotropy. As a potential material, it is important to characterize the anisotropy of the mechanical properties of Ga-Mg compounds. In this work, six number of indices, including the universal anisotropy index (A_U), the percent anisotropy index (A_B and

Table 3. The bulk modulus (B , in GPa), shear modulus (G , in GPa), Yong's modulus (E , in GPa),poisson's ratio (σ , in GPa), the first order Lamé constant (λ , in GPa), the second Lamé constant (μ , in GPa) and the Vickers hardness (H_v , in GPa) of Ga-Mg system.

Species	α -Mg	Ga ₂ Mg ₅	GaMg ₂	GaMg	H-Ga ₂ Mg	O-Ga ₂ Mg	Ga ₅ Mg ₂	α -Ga
B_V	34.2	46.3	48.3	53.3	60.2	56.3	60.3	59.5
B_R	34.2	46.1	47.9	53.1	59.9	56.1	60.3	58.6
B	34.2	46.2	48.1	53.2	60.1	56.2	60.3	59.1
G_V	41.0	29.2	26.3	30.6	44.7	23.1	41.5	26.9
G_R	39.0	28.2	26.1	29.1	40.7	18.3	39.8	20.9
G	40.0	28.7	26.2	29.8	42.7	20.7	40.6	23.9
E	86.3	71.3	66.5	75.3	103.6	55.3	99.5	63.2
B/G	0.86	1.61	1.84	1.78	1.41	2.71	1.49	2.47
σ	0.08	0.24	0.27	0.26	0.21	0.34	0.23	0.32
λ	7.53	27.1	30.6	33.3	31.6	42.4	33.2	43.2
μ	40	28.7	26.2	29.8	42.7	20.7	40.6	23.9
H_v	17.8	5.16	3.64	4.39	9.05	0.66	7.99	1.44

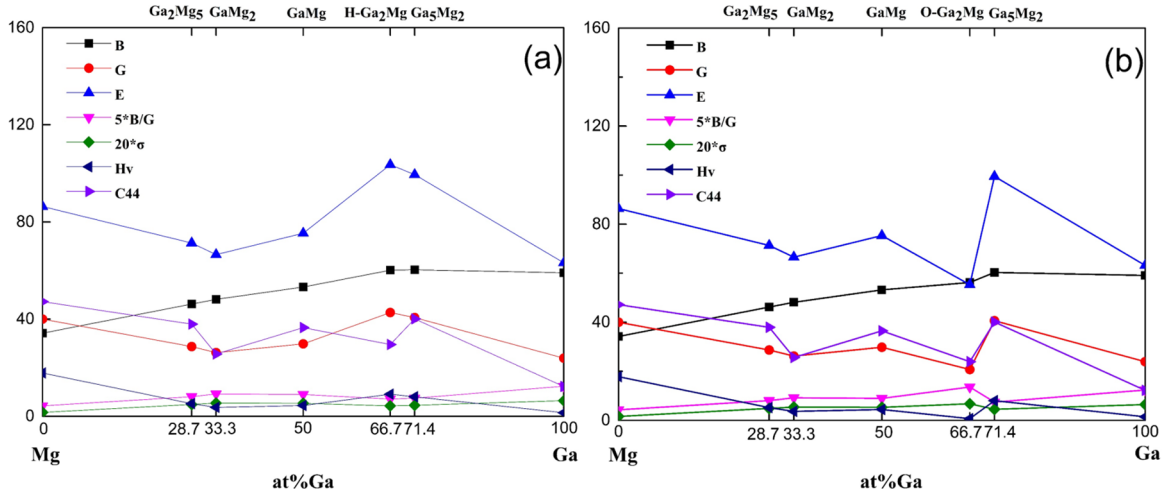


Figure 4. The variations of the elastic parameters of Ga-Mg compounds, note that B/G value is magnified by 5 times and σ value is magnified by 20 times to the initial value.

A_G) and the shear anisotropy factors (A_1 , A_2 and A_3), are obtained by the following equations^{54,55}:

$$A_1 = \frac{4C_{44}}{c_{11} + c_{33} - 2c_{13}} \text{ for (100) plane} \quad (14)$$

$$A_2 = \frac{4C_{55}}{c_{22} + c_{33} - 2c_{23}} \text{ for (100) plane} \quad (15)$$

$$A_3 = \frac{4C_{66}}{c_{11} + c_{22} - 2c_{12}} \text{ for (100) plane} \quad (16)$$

$$A^U = 5 \frac{G_V}{G_R} + \frac{B_V}{B_R} - 6 \geq 0 \quad (17)$$

$$A_B = \frac{B_V - B_R}{B_V + B_R} \quad (18)$$

$$A_G = \frac{G_V - G_R}{G_V + G_R} \quad (19)$$

Where B_V , B_R , G_V and G_R are the bulk and shear modulus estimation within Voigt and Reuss methods, respectively. The values of unity for shear anisotropic factors indicate isotropic for a crystal, while the non-unity values imply anisotropy. The calculated results are shown in Table 4. The A_B value for Ga_5Mg_2 is zero and GaMg_2 has the largest value as 0.41% in Ga_xMg_y compounds, which indicating that the anisotropy in bulk modulus of GaMg_2 is the strongest; But the index A_B is not enough to identify the anisotropy, the index A_U is considered as a better indicator than other indices, which can provide unique and consistent results for the mechanical anisotropic properties of Ga-Mg compounds. Obviously, the lowest A_U value of GaMg_2 in Ga-Mg binary compounds, indicates the elastic modulus of GaMg_2 is not strongly dependent on the different orientations, and it is

confirmed by the following A_G value. In addition, besides α -Ga having the largest A_G and A_U as 12.6% and 1.45 respectively, the largest A_U value for O- Ga_2Mg in binary compounds, suggest that O- Ga_2Mg has the highest elastic anisotropy among the six Ga-Mg binary compounds. The anisotropy of the shear modulus is determined by A_G , A_1 , A_2 and A_3 , and A_1 , A_2 and A_3 represent the anisotropy of the shear modulus in different crystal plane. H- Ga_2Mg has the weakest anisotropy of the shear modulus in (100) plane and (010) plane, and A_1 and A_2 are 0.5, 0.5 respectively. The A_3 values of H- Ga_2Mg , GaMg_2 and GaMg are 1.0, 1.0 and 0.72 respectively. H- Ga_2Mg and GaMg_2 has the same anisotropy of the shear modulus in (001) plane and GaMg has the lowest anisotropy of the shear modulus in (001) plane among all the Ga_xMg_y compounds.

Hexagonal crystal:

$$\frac{1}{B} = (S_{11} + S_{12} + S_{13}) - (S_{11} + S_{12} - S_{13} - S_{33})l_3^2 \quad (20)$$

$$\frac{1}{E} = (1 - l_3^2)S_{11} + l_3^4 S_{33} + l_3^2 (1 - l_3^2)(2S_{13} + S_{44}) \quad (21)$$

Orthorhombic crystal:

$$\frac{1}{B} = (S_{11} + S_{12} + S_{13})l_1^2 + (S_{12} + S_{22} + S_{23})l_2^2 + (S_{13} + S_{23} + S_{33})l_3^2 \quad (22)$$

$$\frac{1}{E} = S_{11}l_1^4 + S_{22}l_2^4 + S_{33}l_3^4 + (2S_{12} + S_{66})l_1^2 l_2^2 + (2S_{13} + S_{55})l_1^2 l_3^2 + (2S_{23} + S_{44})l_2^2 l_3^2 \quad (23)$$

Where S_{ij} are the elastic compliance constants, and l_1 , l_2 and l_3 are the directional cosines. For tetragonal crystal, the above equations (22) and (23) are also suitable by assuming $S_{11} = S_{22}$, $S_{44} = S_{55}$, and $S_{13} = S_{23}$. After substituting the relationships of the direction cosines in spherical coordinates

with respect to θ and φ ($l_1 = \sin\theta \cos\varphi$, $l_2 = \sin\theta \sin\varphi$, $l_3 = \cos\theta$) into equations (22) and (23), we can obtain the projections of surface contour of bulk and Young's modulus shown in Fig.5 and Fig.6. From Fig.5, the projections on the (001), (100) and (110) planes show details about the anisotropic properties of bulk modulus. It is obvious that the bulk modulus of H-Ga₂Mg and O-Ga₂Mg have a strong directional dependence. The bulk modulus of O-Ga₂Mg in the [010] direction is larger than those in the [100] direction and [001] direction on (100) plane, which is in good agreement with the result of calculated elastic constants in which C_{22} is much larger than C_{11} and C_{33} . Meanwhile, For GaMg₂, the bulk modulus in the [001] direction is smaller than those in the [010] and [100] directions, because the value of C_{33} is lower than C_{11} and C_{22} . GaMg₂ has the relatively strong anisotropy and the results are in good agreement with A_B values. From the projections on the (001), (100) and (110)

planes, we find that anisotropy of bulk modulus of GaMg₂ on (001) plane is stronger than that on (100) and (110) plane, but the result is in reverse for GaMg. On the other hand, it is evidence that the bulk modulus of these compounds show weak anisotropy because the planar projections of the gallium magnesium are all close to an ellipsoid.

From Fig.6, The Young's modulus on the (001), (100) and (110) planes show more anisotropic features than the bulk modulus due to the remarkable anisotropic geometry of the projections. Projections deviated from the regular ellipses on the (001), (100) and (110) planes indicate the strong anisotropy of Young's modulus for all the compounds. We may infer that the surface profiles of Young's modulus are anisotropic because their shapes deviate from the ideal sphere. In addition, the Young's modulus of H-Ga₂Mg shows the strongly anisotropy of mechanical properties in Ga-Mg binary compounds. For GaMg, the anisotropy of Young's

Table 4. The calculated universal anisotropic index (A^U), percent anisotropy (A_B and A_G) and shear anisotropic factors (A_1 , A_2 and A_3) of Ga-Mg system.

Species	A_1	A_2	A_3	A_B	A_G	A^U
α -Mg	1.05	1.05	1	0.06%	2.62%	0.2704
Ga ₂ Mg ₅	1.35	1.33	0.79	0.26%	1.82%	0.191251
GaMg ₂	1.04	1.04	1.00	0.41%	0.38%	0.046665
GaMg	1.27	1.27	0.72	0.19%	2.51%	0.261498
H-Ga ₂ Mg	0.50	0.50	1.00	0.25%	4.68%	0.496409
O-Ga ₂ Mg	2.81	0.79	1.20	0.18%	11.59%	1.31504
Ga ₃ Mg ₂	0.76	0.76	1.03	0	2.09%	0.214562
α -Ga	0.24	0.63	0.40	0.76%	12.6%	1.450765

The most straightforward way to describe the elastic anisotropy is to plot the bulk and Young's modulus in two dimensions (2D) as a function of the crystallographic direction. The directional dependence of bulk and Young's modulus is given by^{56,57}

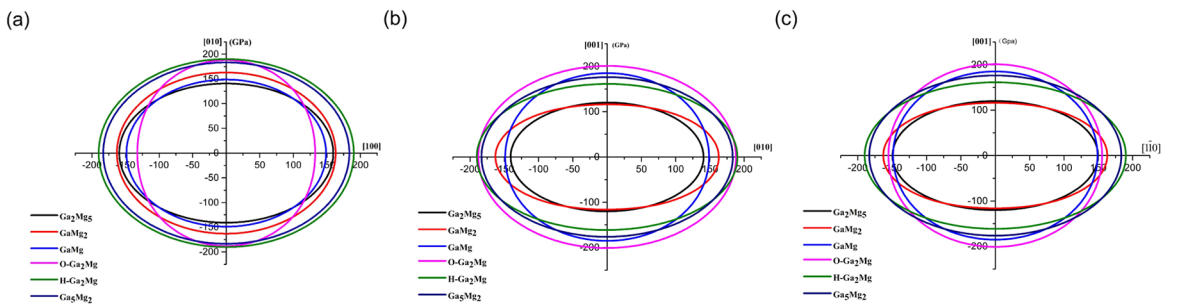


Figure 5. (a)-(c) The (001), (100) and (110) planar projections of the bulk modulus of Ga_xMg_y compounds, respectively.

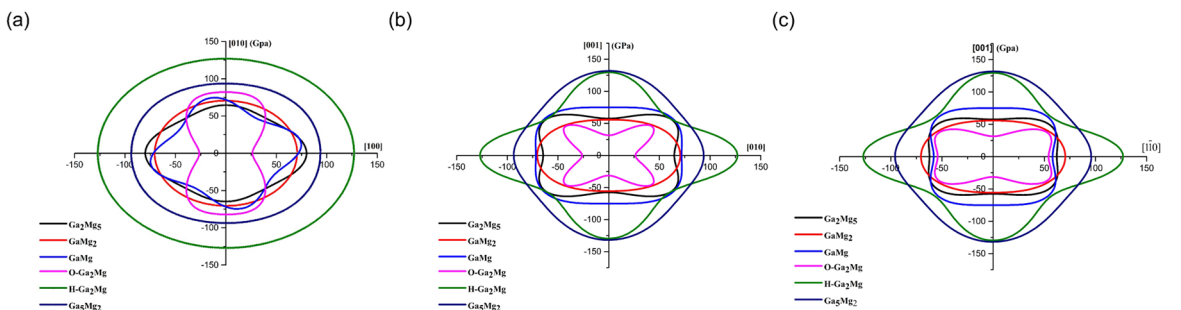


Figure 6. (a)-(c) The (001), (100) and (110) planar projections of the Young's modulus of Ga_xMg_y compounds, respectively.

modulus on (100) plane is weaker than that on (001) plane thus the projection on (001) plane is strongly polarized, and the anisotropy of Young's modulus for H-Ga₂Mg on (001) plane is weaker than that on (100) plane and the projection on (100) plane is strongly polarized, H-Ga₂Mg shows the maximum Young's modulus along [010] and the value of Young's modulus in [100] direction are also larger than other compounds on (001) plane. In addition, GaMg₂ and H-Ga₂Mg on the plane (100) are similar to those on the plane (110), which implies the analogous anisotropy of Young's modulus on these planes. Obviously, O-Ga₂Mg shows the minimum Young's modulus along the [001] direction. It can also be found that Ga₂Mg₃ and O-Ga₂Mg show the weakest anisotropy for Young's modulus on (001) and (010) planes, respectively.

3.4 Anisotropic sound velocity

The average sound velocity v_m is calculated by^{58,59}:

$$v_m = \left[\frac{1}{3} \left(\frac{2}{v_l^3} + \frac{1}{v_t^3} \right) \right]^{-1/3} \quad (24)$$

v_l and v_t are the longitudinal sound velocity and transverse sound velocity, respectively.

The following equations were used to calculate the bulk modulus (B) and shear modulus (G) previously obtained⁶⁰.

$$v_l = \sqrt{\frac{(B + (4/3)G)}{\rho}} \quad (25)$$

$$v_t = \sqrt{\frac{G}{\rho}} \quad (26)$$

Table 5 shows the calculated acoustic velocities of Ga-Mg binary compounds. Ga₂Mg₃ has the largest acoustic velocity among Ga-Mg binary compounds because it has the largest shear modulus and lowest density.

The acoustic velocity in a crystal is anisotropic which is determined by the symmetry of the crystal and propagation directions⁵⁴. For example, the pure transverse and longitudinal modes can only be found for [100], [001] and [110] directions in a tetragonal crystal and the sound propagating modes in

other directions are the quasi-transverse or quasi-longitudinal waves. In this work, we only consider the pure propagating modes for Ga_xMg_y compounds and the acoustic velocities in the principal directions can be simply expressed as^{61,62}:

Tetragonal crystal:

$$\begin{aligned} [100] &= [010] \\ [100]v_l &= \sqrt{C_{11}/\rho}; [001]v_{t1} = \sqrt{C_{44}/\rho}; \\ [010]v_{t2} &= \sqrt{C_{66}/\rho} \end{aligned} \quad (27)$$

$$\begin{aligned} [001] \\ [001]v_l &= \sqrt{C_{33}/\rho}; [100]v_{t1} = [010]v_{t2} = \sqrt{C_{66}/\rho} \end{aligned} \quad (28)$$

$$\begin{aligned} [110] \\ [110]v_l &= \sqrt{(C_{11} + C_{12} + 2C_{66})/2\rho}; \\ [001]v_{t1} &= \sqrt{C_{44}/\rho}; [1\bar{1}0]v_{t2} = \sqrt{(C_{11} - C_{12})/2\rho} \end{aligned} \quad (29)$$

Orthorhombic crystal:

$$\begin{aligned} [100] \\ [100]v_l &= \sqrt{C_{11}/\rho}; [010]v_{t1} = \sqrt{C_{66}/\rho}; \\ [001]v_{t2} &= \sqrt{C_{55}/2\rho} \end{aligned} \quad (30)$$

$$\begin{aligned} [010] \\ [010]v_l &= \sqrt{C_{22}/\rho}; [100]v_{t1} = \sqrt{C_{66}/\rho}; \\ [001]v_{t2} &= \sqrt{C_{44}/\rho} \end{aligned} \quad (31)$$

$$\begin{aligned} [001] \\ [001]v_l &= \sqrt{C_{33}/\rho}; [010]v_{t1} = \sqrt{C_{55}/\rho}; \\ [010]v_{t2} &= \sqrt{C_{44}/\rho} \end{aligned} \quad (32)$$

Hexagonal crystal:

$$\begin{aligned} [100] \\ [100]v_l &= \sqrt{(C_{11} - C_{12})/\rho}; [010]v_{t1} = \sqrt{C_{11}/\rho}; \\ [001]v_{t2} &= \sqrt{C_{44}/\rho} \end{aligned} \quad (33)$$

$$\begin{aligned} [001] \\ [001]v_l &= \sqrt{C_{33}/\rho}; [100]v_{t1} = \sqrt{C_{44}/\rho}; \\ [010]v_{t2} &= \sqrt{C_{44}/\rho} \end{aligned} \quad (34)$$

Table 5. The theoretical density (ρ , g/cm³), longitudinal sound velocity (v_l , m/s), shear sound velocity (v_t , m/s), average sound velocity (v_m , m/s) of Ga_xMg_y.

Species	ρ	v_l	v_t	v_m
α -Mg	1.74	7092.7	4794.6	5890.5
Ga ₂ Mg ₃	3.03	5279.8	3077.6	3271.5
GaMg ₂	3.27	5039.1	2830.6	3689.7
GaMg	4.07	4778.5	2705.9	3519.7
H-Ga ₂ Mg	4.92	4877.2	2946.0	3761.9
O-Ga ₂ Mg	6.41	4152.0	2063.5	2766.2
Ga ₃ Mg ₂	5.05	4760.3	2835.4	3636.0
α -Ga	6.41	3767.1	1930.9	2572.1

Where v_{t1} is the first transverse mode and v_{t2} is the second transverse mode. The calculated results are presented in Table 6 and 7. The anisotropy of acoustic velocities also reveals the elastic anisotropy in these crystals. Some anisotropic, including sound velocity in different direction, can be expressed by C_{ij} , that is, C_{ij} in different direction represents different sound velocity. Thus, the more modulus of the direction, the higher speed of the sound. For example, the C_{11} , C_{22} and C_{33} determine the longitudinal sound velocities along [100], [010] and [001] directions, respectively, and C_{44} , C_{55} and C_{66} correspond to the transverse modes.

Table 6. The anisotropic sound velocities of tetragonal Ga₃Mg₂ and GaMg compounds. The unit of velocity (v) is km/s.

Direction	[100]			[001]			[110]		
	[100]v _l	[001]v _{tl}	[010]v _{t2}	[001]v _l	[100]v _{tl}	[010]v _{t2}	[110]v _l	[001]v _{tl}	[110]v _{t2}
Ga ₃ Mg ₂	4.764	2.818	2.618	5.210	2.618	2.618	4.788	2.818	2.576
GaMg	4.705	2.995	2.309	4.862	2.309	2.309	4.482	2.995	2.717

Table 7. The anisotropic sound velocities of orthorhombic O-Ga₂Mg, Ga₂Mg₃ and hexagonal GaMg₂, H-Ga₂Mg compounds. The unit of velocity (v) is km/s.

Direction	[100]			[010]			[001]		
	[100]v _l	[010]v _{tl}	[001]v _{t2}	[010]v _l	[100]v _{tl}	[001]v _{t2}	[001]v _l	[100]v _{tl}	[010]v _{t2}
O-Ga ₂ Mg	3.770	2.455	2.132	4.596	2.455	2.216	4.005	2.132	2.216
Ga ₂ Mg ₃	5.549	2.809	3.159	5.162	2.809	3.535	4.908	3.159	3.535
GaMg ₂	2.951	5.193	2.798	--	--	--	4.689	2.798	2.798
H-Ga ₂ Mg	3.233	5.275	2.449	--	--	--	5.199	2.449	2.449

4. Conclusions

In summary, the chemical stability, elastic properties, anisotropy of mechanical properties and anisotropic sound velocity of the Ga-Mg binary compounds have been investigated by first principles calculations. The cohesive energy and formation enthalpy of Ga_xMg_y compounds show that the compounds are thermodynamically stable, GaMg is the most stable compound and has the lowest formation enthalpy with -0.1621eV/atom in Ga-Mg binary system, which is in good agreement with the experimental values. Ga₃Mg₂ and H-Ga₂Mg have the larger bulk, shear and Young's modulus as 60.3, 40.6 99.5 GPa and 60.1, 42.7, 103.6 GPa, respectively, and corresponding B/G is small. The results of Poisson's ratio varies from 0.21 for H-Ga₂Mg to 0.34 for O-Ga₂Mg, the lowest values of H-Ga₂Mg imply that it is harder than other compounds. The Young's modulus of H-Ga₂Mg shows the strongly anisotropy of mechanical properties and that of GaMg₂, the weakest anisotropy among all the compounds. Moreover, the hardness of Ga-Mg binary system is evaluated from 0.66 to 9.05 GPa. The results of anisotropic sound velocities showed C_{11} , C_{22} and C_{33} determine the longitudinal sound velocities along [100], [010] and [001] directions, respectively, and C_{44} , C_{55} and C_{66} correspond to the transverse modes. The results are helpful for the experiment design and application of Ga-Mg binary compounds in the future.

5. Acknowledgements

Project supported by Natural Science Foundation of Hunan province, China (2017JJ5040).

6. References

- Ma KQ, Liu J. Heat-driven liquid metal cooling device for the thermal management of a computer chip. *Journal of Physics D: Applied Physics*. 2007;40(15):4722-4729.
- Deng YG, Liu J. A liquid metal cooling system for the thermal management of high power LEDs. *International Communications in Heat and Mass Transfer*. 2010;37(7):788-791.
- Deng Y, Liu J. Hybrid liquid metal-water cooling system for heat dissipation of high power density microdevices. *Heat and Mass Transfer*. 2010;46(11-12):1327-1334
- Vetrovec J, Litt AS, Copeland DA, Junghans J, Durkee R. *Liquid metal heat sink for high-power laser diodes*. In: Proceedings of SPIE - The International Society for Optical Engineering; 2013 Feb 2-7; San Francisco, CA, USA. 8605:8605E-1-7.
- Dai D, Zhou YX, Liu J. Liquid metal based thermoelectric generation system for waste heat recovery. *Renewable Energy*. 2011;36(12):3530-3536.
- Liu J, Li HY, inventors. *A Thermal Energy Harvesting Device and its Fabrication Method*. China Patent 201210241718.0. 2012.
- Kim HJ, Son C, Ziaie B. A multiaxial stretchable interconnect using liquid-alloy-filled elastomeric microchannels. *Applied Physics Letters*. 2008;92(1):11904.
- Cao A, Yuen P, Lin L. Microrelays With Bidirectional Electrothermal Electromagnetic Actuators and Liquid Metal Wetted Contacts. *Journal of Microelectromechanical Systems*. 2007;16(3):700-708.
- Knoblauch M, Hibberd JM, Gray JC, van Bel AJ. A galinstan expansion femtosyringe for microinjection of eukaryotic organelles and prokaryotes. *Nature Biotechnology*. 1999;17(9):906-909.
- Liu J, inventor. *Piezoelectric Thin Film Electricity Generator and its Fabrication Method*. China Patent 2012103225845. 2012.
- Gao YX, Liu J. Gallium-based thermal interface material with high compliance and wettability. *Applied Physics A*. 2012;107(3):701-708.
- Zhang Q, Liu J. Nano liquid metal as an emerging functional material in energy management, conversion and storage. *Nano Energy*. 2013;2(5):863-872.
- Zhang Q, Zheng Y, Liu J. Direct writing of electronics based on alloy and metal (DREAM) ink: A newly emerging area and its impact on energy, environment and health sciences. *Frontiers in Energy*. 2012;6(4):311-340.

14. Gao Y, Li H, Liu J. Direct Writing of Flexible Electronics through Room Temperature Liquid Metal Ink. *PLoS One*. 2012;7(9):e45485.
15. Jeong SH, Hagman A, Hjort K, Jobs M, Sundqvist J, Wu Z. Liquid alloy printing of microfluidic stretchable electronics. *Lab on a Chip*. 2012;12(22):4657-4664.
16. Zheng Y, He Z, Gao Y, Liu J. Direct Desktop Printed-Circuits-on-Paper Flexible Electronics. *Scientific Reports*. 2013;3:1786-1792.
17. Taccardi N, Grabau M, Debuschewitz J, Distaso M, Brandl M, Hock R, et al. Gallium-rich Pd-Ga phases as supported liquid metal catalysts. *Nature Chemistry*. 2017;9:862-867.
18. Feng Y, Wang R, Peng C. Influence of Ga and In on microstructure and electrochemical properties of Mg anodes. *Transactions of Nonferrous Metals Society of China*. 2013;23(9):2650-2656.
19. Zhao J, Yu K, Hu Y, Li S, Tan X, Chen F, et al. Discharge behavior of Mg-4wt%Ga-2 wt%Hg alloy as anode for seawater activated battery. *Electrochimica Acta*. 2011;56(24):8224-8231.
20. Wu D, Ouyang L, Wu C, Wang H, Liu J, Sun L, et al. Phase transition and hydrogen storage properties of Mg-Ga alloy. *Journal of Alloys and Compounds*. 2015;642:180-184.
21. Xin Y, Hu T, Chu PK. Influence of test solutions on in vitro studies of biomedical magnesium alloys. *Journal of Electrochemical Society*. 2010;157(7):238-243.
22. Virtanen S. Biodegradable Mg and Mg alloys: Corrosion and biocompatibility. *Materials Science and Engineering: B*. 2011;176(20):1600-1608.
23. Mohedano M, Blawert C, Yasakau KA, Arrabal R, Matykina E, Mingo B, et al. Characterization and corrosion behavior of binary Mg-Ga alloys. *Materials Characterization*. 2017;128:85-89.
24. Predel B, Stein DW. Thermodynamic Investigation of the Gallium-Magnesium System. *Journal of the Less Common Metals*. 1969;18(3):203-213.
25. Nayeb-Hashemi AA, Clark JB. The Ga-Mg (Gallium-Magnesium) system. *Bulletin of Alloy Phase Diagrams*. 1985;6(5):434-439.
26. Feng Y, Wang RC, Liu HS, Jin ZP. Thermodynamic reassessment of the magnesium-gallium system. *Journal of Alloys and Compounds*. 2009;486(1-2):581-585.
27. Meng FG, Wang J, Rong MH, Liu LB, Jin ZP. Thermodynamic assessment of Mg-Ga binary system. *Transactions of Nonferrous Metals Society of China*. 2010;20(3):450-457.
28. Zhang H, Shang S, Saal JE, Saengdeejing A, Wang Y, Chen LQ, et al. Enthalpies of formation of magnesium compounds from first-principles calculations. *Intermetallics*. 2009;17(11):878-885.
29. Hohenberg P, Kohn W. Inhomogeneous Electron Gas. *Physical Review*. 1964;136(3B):864-871.
30. Segall MD, Lindan PJD, Probert MJ, Pickard CJ, Hasnip PJ, Clark SJ, et al. First-principles simulation: ideas, illustrations and the CASTEP code. *Journal of Physics: Condensed Matter*. 2002;14(11):2717-2744.
31. Kresse G, Joubert D. From ultrasoft pseudopotentials to the projector augmented-wave method. *Physical Review B*. 1999;59(3):1758-1775.
32. Perdew JP, Burke K, Ernzerhof M. Generalized Gradient Approximation Made Simple. *Physical Review Letters*. 1996;77(18):3865-3868.
33. Monkhorst HJ, Pack JD. Special points for Brillouin-zone integrations. *Physical Review B*. 1976;13(12):5188-5192.
34. Feng J, Xiao B, Chen JC, Du Y, Yu J, Zhou R. Stability, thermal and mechanical properties of PtxAly compounds. *Materials & Design*. 2011;32(6):3231-3239.
35. Okamoto H. Ga-Mg (Gallium-Magnesium). *Journal of Phase Equilibria and Diffusion*. 2013;34(2):148.
36. Ellner M, Gödecke T, Duddek G, Predel B. Strukturelle und konstitutionelle Untersuchungen im galliumreichen Teil des Systems Magnesium-Gallium. *Zeitschrift für anorganische und allgemeine Chemie*. 1980;463(1):170-178.
37. Rossini FD. *Selected values of chemical thermodynamic properties*. Washington: United States National Bureau of Standards Publishing; 1965.
38. Nayeb-Hashemi AA, Clark JB. *Phase diagrams of binary magnesium alloys*. Materials Park: ASM International; 1988.
39. Smith GS, Mucker KF, Johnson Q, Wood DH. The crystal structure of Ga₂Mg. *Acta Crystallographica*. 1969;B25:549-553.
40. Smith GS, Mucker KF, Johnson Q, Wood DH. Crystal structure of Ga₃Mg₂. *Acta Crystallographica*. 1969;B25:554-557.
41. Schubert K, Gauzzi F, Frank K. Kristallstruktur Einiger Mg-B-3-phasen. *Zeitschrift für Metallkunde*. 1963;54(7):422-429.
42. Frank K, Schubert K. Kristallstruktur von Mg₂Ga und Mg₂Ti. *Journal of the Less-Common Metals*. 1970;20(3):215-221.
43. Schubert K, Frank K, Gohle R, Maldonado A, Meissner HG, Raman A, Rossteutscher W. *Naturwissenschaftliche*. 1963;50(2):41.
44. von Ellner M, Goedecke T, Duddek G, Predel B. Structure and Constitutional Studies in the Gallium-Rich Part of the Magnesium-Gallium System. *Zeitschrift für Anorganische und Allgemeine Chemie*. 1980;463:170-178.
45. Han J, Wang C, Liu X, Wang Y, Liu ZK, Jiang J. Atomic-Level Mechanisms of Nucleation of Pure Liquid Metals during Rapid Cooling. *Chemphyschem*. 2015;16(18):3916-3927.
46. Wu ZJ, Zhao EJ, Xiang HP, Hao XF, Liu XJ, Meng J. Crystal structures and elastic properties of superhard IrN₂ and IrN₃ from first principles. *Physical Review B*. 2007;76(5-1):054115.
47. Reuss A, Angew Z. Calculation of the flow limits of mixed crystals on the basis of the plasticity of monocrystals. *Zeitschrift für Angewandte Mathematik und Mechanik*. 1929;9:49-58.
48. Hill R. The elastic behaviour of a crystalline aggregate. *Proceedings of the Physical Society, Section A*. 1952;65(5):349-354.
49. Chong XY, Jiang YH, Zhou R, Feng J. Electronic structures mechanical and thermal properties of V-C binary compounds. *RSC Advances*. 2014;4(85):44959-44971.
50. Chong XY, Jiang YH, Zhou R, Feng J. The effects of ordered carbon vacancies on stability and thermo-mechanical properties of V8C7 compared with VC. *Scientific Reports*. 2016;6:34007-34016.
51. Gao F. Hardness estimation of complex oxide materials. *Physical Review B*. 2004;69(9):094113-094113.
52. Jiang X, Zhao J, Jiang X. Correlation between hardness and elastic moduli of the covalent crystals. *Computational Materials Science*. 2011;50(7):2287-2290.

53. Chen XQ, Niu H, Li D, Li Y. Modeling hardness of polycrystalline materials and bulk metallic glasses. *Intermetallics*. 2011;19(9):1275-1281.
54. Feng J, Xiao B, Zhou R, Pan W, Clarke DR. Anisotropic elastic and thermal properties of the double perovskite slab-rock salt layer Ln₂SrAl₂O₇ (Ln= La, Nd, Sm, Eu, Gd or Dy) natural superlattice structure. *Acta Materialia*. 2012;60(8):3380-3392.
55. Xiao B, Feng J, Zhou CT, Jiang YH. Mechanical properties and chemical bonding characteristics of Cr₇C₃ type multicomponent carbides. *Journal of Applied Physics*. 2011;109(2):023507.
56. Panda KB, Chandran KSR. First principles determination of elastic constants and chemical bonding of titanium boride (TiB) on the basis of density functional theory. *Acta Materialia*. 2006;54(6):1641-1657.
57. Chong XY, Jiang YH, Zhou R, Feng J. Elastic properties and electronic structures of Cr_xBy as superhard compounds. *Journal of Alloys and Compounds*. 2014;610:684-694.
58. Kittel C, McEuen P. *Introduction to Solid State Physics*. New York: Wiley Publishing; 1986.
59. Chong XY, Jiang YH, Feng J. Mechanical properties, electronic structure and alkali-ion diffusion of Eldfellite-type AFe(SO₄)₂ (A=LiA=Li, Na, K) as potential cathode materials comparing with LiFePO₄. *Journal of Micromechanics and Molecular Physics*. 2017;2(1):1750002.
60. Chong XY, Jiang YH, Zhou R, Feng J. First principles study the stability, mechanical and electronic properties of manganese carbides. *Computational Materials Science*. 2014;87:19-25.
61. Hearmon RFS. *An Introduction to Applied Anisotropic Elasticity*. London: Oxford University Press; 1961.
62. Chong XY, Jiang YH, Zhou R, Feng J. Stability, chemical bonding behavior, elastic properties and lattice thermal conductivity of molybdenum and tungsten borides under hydrostatic pressure. *Ceramics International*. 2015;42(2):2117-2132.